Accepted Manuscript

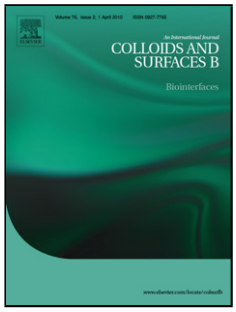

Title: Facile Fabrication of P(OVNG-*co*-NVCL) Thermoresponsive Double-Hydrophilic Glycopolymer Nanofibers for Sustained Drug Release

Author: Mu-Ru Xu co-first Meng Shi co-first David H Bremner Kan Sun Hua-Li Nie Jing Quan Li-Min Zhu

PII: S0927-7765(15)30075-8
DOI: http://dx.doi.org/doi:10.1016/j.colsurfb.2015.07.041
Reference: COLSUB 7245

To appear in: *Colloids and Surfaces B: Biointerfaces*

Received date: 23-3-2015
Revised date: 26-6-2015
Accepted date: 16-7-2015

Please cite this article as: Mu-Ru Xu co-first, Meng Shi co-first, David H Bremner, Kan Sun, Hua-Li Nie, Jing Quan, Li-Min Zhu, Facile Fabrication of P(OVNG-co-NVCL) Thermoresponsive Double-Hydrophilic Glycopolymer Nanofibers for Sustained Drug Release, Colloids and Surfaces B: Biointerfaces http://dx.doi.org/10.1016/j.colsurfb.2015.07.041

Facile Fabrication of P(OVNG-*co*-NVCL) Thermoresponsive Double-Hydrophilic Glycopolymer Nanofibers for Sustained Drug Release

Mu-Ru Xu (co-first)[1], *Meng Shi (co-first)*[1], *David H Bremner* [2], *Kan Sun*[1], *Hua-Li Nie*[1], *Jing Quan*[*1], *Li-Min Zhu*[*1]

[1,] *College of Chemistry, Chemical Engineering and Biotechnology, Donghua University, Shanghai, 201620, P.R. China.*

[2,] *School of Science, Engineering and Technology, Kydd Building, Abertay University, Dundee DD1 1HG, Scotland, UK*

Highlights

1. Thermoresponsive double hydrophilic copolymers are one of the most important candidates of biomaterials and have capability of reversible micellization and dissociation responding to the change of temperature.
2. We prepared thermoresponsive double-hydrophilic glycopolymers (TDHG) nanofibers for the first time by a free radical copolymerization and electrospinning method.
3. The cytotoxicity of TDHG nanofibers were investigated for their potential as drug carriers in controlled drug delivery for targeting of hepatic cells.

Graphical abstract “cluster-glycoside effect” of PNA-FITC and P(OVNG-*co*-NVCL)

Abstract

The thermoresponsive double-hydrophilic glycopolymer (DHG), Poly

(6-O-vinyl-nonanedioyl-D-galactose-*co*-N-vinylcaprolactam) (P(OVNG-*co*-NVCL)) was synthesized via a chemo-enzymatic process and a free radical copolymerization and the resulting nanofibers were fabricated using an electrospinning process. The desired lower critical solution temperature (LCST) between 32 and 40 ^{o}C of the DHG polymers was achieved by adjusting the molar fraction of galactose monomer in the copolymers during the synthesis. The thermoresponsive DHG polymers were found to have good cytocompatibility with Hela cells as determined by the MTT assay, and special recognition of the protein peanut agglutinin (PNA). The drug release properties of these newly designed thermoresponsive DHG P(OVNG-*co*-NVCL) nanofibers are temperature regulated, can target specific proteins and have the potential application in the field of sustained drug release.

Keywords: thermoresponsive, glycopolymer, sustained release, drug loaded nanofiber, lectin binding

Corresponding author: Jing Quan, College of Chemistry, Chemical Engineering and Biotechnology, Donghua University, Shanghai, 201620, P.R. China.

Corresponding author: Li-Min Zhu, College of Chemistry, Chemical Engineering and Biotechnology, Donghua University, Shanghai, 201620, P.R. China.

Telephone numbers: +86021-67792748 (Jing Quan), +86021-67792655(Li-Min Zhu).

E-mail addresses: jquan@dhu.edu.cn (Jing Quan), lzhu@dhu.edu.cn (Li-Min Zhu).

1. Introduction

Stimuli-responsive polymer nanocarriers are widely used in controlled-release systems [1-2]. These materials may change their affinity for water so that interior channels open or close in response to external stimuli such as temperature or pH change [3]. Thermoresponsive double hydrophilic copolymers are one of the most important types of biomaterials and have the capability of reversible micellization and dissociation responding to the change of temperature [4]. These copolymers, containing at least one functional unit such as temperature-responsive, light-sensitive and pH-sensitive monomers, have recently attracted significant interest for potential applications in drug delivery systems [5-6]. Thus, novel double hydrophilic polymers have been developed which can undergo a reversible change of morphology in response to the environmental stimuli to provide smart therapy with active drugs [7].

In order to modify functionality, to produce smart stimuli-responsive copolymers with bioactive molecules, much attention has been focused on the fabrication of glycopolymers due to their biocompatibility, biodegradability and the hydrophilic nature of the carbohydrate moieties [8-9]. The glycopolymers have been used to mimic biological systems such as binding lectins through multipoint interactions [10]. In our previous research, thermoresponsive double hydrophilic glycopolymers have been investigated and these glycopolymers have shown promising capability for protein binding [11].

Recent advances in micro and nanotechnology show that polymer microparticles or nanoparticles (NPs), micelles, nanogels, liposomes, dendrimers, and composite nanofibers can be used for drug delivery applications [12]. Compared with the

nanoparticulate systems, electrospun nanofibrous scaffolds have high specific surface areas, high porosity, and three-dimensional network structures which can, for instance, enhance the adhesion, the proliferation and growth of cells [13]. In addition, using tissue engineering, the fibers can also be used as carriers in controlled drug release, delivering prolonged or better targeted drug delivery [14]. To the best of our knowledge, few reports relating to the thermoresponsive double hydrophilic glycopolymers nanofibers for drug controlled release are available.

In this work, thermoresponsive double-hydrophilic glycopolymeric (TDHG) nanofibers were prepared using free radical copolymerization and electrospinning methodology [15]. Drug-loaded TDHG nanofibers were also prepared in order to investigate the influence of temperature, pH and the nature of the polymer on drug release [16]. The cytotoxicity of TDHG nanofibers were also investigated for their potential as drug carriers in controlled drug delivery for targeting hepatic cells.

2. Materials and methods

2.1 Materials

N-vinyl caprolactam (NVCL) and Phosphate Buffered Saline (PBS) (0.01 M, pH 7.4) were purchased from Sigma-Aldrich (Shanghai) Trading Co., Ltd. Alkaline protease from Bacillus subtilis (EC 3.1.1.3, powder, a crude preparation of alkaline serine protease, powder, 200 u/mg) was acquired from the Wuxi Xuemei Technology Co. Fluorescein isothiocyanate (FITC), bovine serum albumin (BSA), peanut agglutinin (PNA) were purchased from Shanghai BioSun Sci & Tech Co., Ltd. Hela

cell, fetal calf serum, trypsin (2.5 g/L) and Dulbecco's modified eagle's medium (DMEM) were acquired from Hang Zhou jinuo bio-pharmaceutical Technology Co., Ltd. Ethyl acetate, azelaic acid, mercuric acetate, copper acetate, petroleum ether, 2,2'-Azo-bis-iso-butyronitrile (AIBN, 97%), methyl alcohol, tetrahydrofuran, pyridine, sodium bicarbonate, sodium carbonate, sodium chloride, and dimethyl sulfoxide (DMSO) were purchased from the China National Medicines Corporation Ltd. (Beijing, China). β-Lactose and calcium chloride were of analytical grade and were purchased from the Sinopharm Chemical Reagent Co., Ltd. All solvents used in this work were of analytical grade and were dried by storing over activated 4 Å molecular sieves for 24 h prior to use. All other reagents were used as received. Water was distilled before use.

2.2 Preparation of P(OVNG-*co*-NVCL)

The polymerizable galactose derivatives, 6-O-vinyl-nonanedioyl-D-galactose (OVNG), were synthesized, using alkaline protease as a catalyst, according to a previously published protocol in anhydrous pyridine at 50 ^{o}C, with stirring at 250 rpm for 3-4 days [17-18]. A series of P(OVNG-*co*-NVCL) were subsequently synthesized in dimethylformamide (DMF) with 2, 2'-azodiisobutyronitrile (AIBN) as an initiator using molar input ratios of OVNG to NVCL of 1:1, 1:4, 1:6, 1:8 (mol/mol). In a typical protocol, OVNG (0.2 g) and NVCL (0.0915 g/0.1489 g) were dissolved in DMF (1.0 mL), AIBN (0.00583 g/0.010978 g, 2% of total mass, w/w) was subsequently added after the two monomers dissolved under an atmosphere of N_2.

The polymerization was carried out at room temperature for 8 h. The resulting products were subjected to three dissolutions (in methanol) – coaguline (by diethyl ether) cycles and then dried under vacuum. Giving a yield of 78%-80%.

Scheme.1

2.3 Characterization

^{1}H NMR measurements were performed on an Advance (Bruker, Rheinstetten, Germany) Unity Plus 400 MHz nuclear magnetic resonance spectrometer using D_2O as the solvent. FT-IR spectra were obtained between 400 and 4500 cm^{-1} on a Nicolet NEXUS-670 (Nicolet Instrument Corporation, WI, USA) at room temperature. The spectra. The number-average molecular weight (*Mn*), weight-average molecular weight (*Mw*), and polydispersity (*Mw/Mn*) of the polymers were determined by gel permeation chromatography (GPC) at 35 ^{o}C using a Waters 1525 chromatograph equipped with a Waters 2414 refractive index detector. Tetrahydrofuran (THF) was used as the mobile phase at a flow rate of 1 mL/min. The GPC columns were standardized with narrow dispersity polystyrene in molecular weights ranging from 4.7×10^{6} to 2350.

Lower critical solution temperature (LCST) measurements

The LCST is defined as the temperature when the solution is reduced to 50% of the transmittance. After a whole band (200-900 nm) wavelength scanning, the transmittance of polymer aqueous solution (1 mg/mL) was determined at λ=226 nm

using a PerkinElmer lambda 35 UV-visible spectrophotometer equipped with a temperature control unit. The heating rate of the product cuvette and the reference cuvette was set as 2 $^{o}C \cdot min^{-1}$.

2.4 Lectin-binding tests

P(OVNG-*co*-NVCL) Glycopolymers have a common structure feature such as galactosyl, which can be studied for the binding interaction between lectin and carbohydrates. A typical procedure is described as follows: a stock solution of P(OVNG-*co*-NVCL) in PBS (pH=7.4) at a concentration of 1.5 mg/mL was added to a solution of FITC-PNA (1.317 mg/mL) in PBS, to which was added $CaCl_2$(1mM), and BSA (1mg) and these were mixed together and kept at 4 ^{o}C for 1 h in the dark, then dialysed in PBS (pH=7.4) for 48 h at room temperature. Images of the FITC-PNA binding to the glycopolymers were recorded using a confocal laser scanning microscope (Carl Zeiss LSM700, Jena, Germany).

2.5 In vitro cytotoxicity studies

Hela cells (Rochen biotechnology, Shanghai, China) were seeded into 96-well plates at a density of 6,000 cells per well, and grown for 24 h. The cells were then incubated with a series of glycopolymers P(OVNG-*co*-NVCL) in different concentrations for 48 h. After washing the cells with PBS buffer, fresh DMEM medium (100 μL) and 10 μL of MTT solution (5 mg/mL) were added to each well and the plates were incubated at 37 ^{o}C for another 3 h. After incubation, the culture

medium was removed and 50 μL of DMSO was added to each well and shaken for 10 min at ambient temperature to make the internalized purple formazan crystals dissolved. The absorbance was measured at a wavelength of 570 nm using a plate reader (MULTSIKANMK3, Thermo USA). Each experiment was conducted in 5 replicates per plate, four plates were used and the results were expressed as a percentage of cell viability.

2.6 Preparation of drug-loaded composite nanofibers

P(OVNG-*co*-NVCL) nanofibrous mats were first prepared without ferulic acid. In order to achieve better fibrous morphologies and diameters, a L_9 (3) ^{4} orthogonal analysis table was used to show conditions, the orthogonal experiment design and analysis were figured out by orthogonal design assistant II V3.1.1. P(OVNG-*co*-NVCL) homogeneous solutions of 35, 37, and 39 wt% were prepared by dissolving P(OVNG-*co*-NVCL) powder in ethanol at ambient temperature under stirring for 12 h. Electrical voltages were set at 12, 13.5, and 15 kV, with three distances (12, 15, and 18 cm) respectively between the syringe tip and the collection. The feed rates of solutions were maintained at 0.3, 0.5, and 0.7 mL/h using a single syringe pump. The electrospinning process was carried out at ambient conditions (ambient temperature, relative humidity of 60±3%). The homogeneous spinning solutions were loaded in a 1 mL syringe fitted with a stainless steel capillary needle with an internal diameter of 0.5 mm and the fibers were collected one a piece of aluminum foil. The fibers were visualized using scanning electron microscopy (SEM;

JSM-5600 LV microscope, JEOL, Tokyo, Japan), and analyzed for average diameters. The best spinning conditions (39 wt%, 12 kV, 18 cm, 0.7 mL/h) were selected so as to form nanofibers with minimum average diameter.

Table 1

P(OVNG-*co*-NVCL) and ferulic acid (FA) were dissolved in ethanol at ambient temperature under gentle stirring overnight, to achieve a homogeneous solution. The concentration of P(OVNG-*co*-NVCL) was fixed at 39 wt%, and fibers were synthesized with different quantities of FA (5%, 10% and 20 wt% FA) in the blend membranes. Drug-loaded P(OVNG-*co*-NVCL) solutions were then used for electrospinning.

2.7 SEM measurements

The surface topology of the glycopolymer nanofibers, before and after drug insertion was analyzed using scanning electron microscopy (S-4800, Japan Hitachi). A sample of about 2 mm^2 was attached to the plate, and the samples were sputter-coated with gold for 30 seconds to improve its electroconductivity. The diameters of the electrospun fibers were analyzed using Image J software using more than 60 images from each sample of fiber.

2.8 TGA analysis

The thermo gravimetric analyses were performed using a TG 209 F1 (TA Instruments Co., DE, USA), in a nitrogen atmosphere and dynamic conditions, over the temperature range from 10 ^{o}C to 900 ^{o}C with a heating rate of 10 ^{o}C/min. The data were collected and processed using a Proteus Analysis data system from Netzsch.

2.9 In vitro release study

In the controlled drug release study ferulic acid (FA) was used as the model drug during the electrospinning procedure. Glycopolymer fibers electrospun from solutions A, B and C, each weighing about 25 mg (encapsulating about 5%, 10% of FA) were soaked in 5 mL of PBS (pH=7.4) in a dialysis bag with PBS (pH=7.4) in glass vials as dialysate. At various times, 3 mL of the supernatant was removed from the vial, and replaced by an equal volume of fresh medium. Drug release was carried out at 20 ^{o}C and 40 ^{o}C separately. The concentrations of FA in supernatant were then monitored using a UV-visible spectrophotometer at an optical wavelength of 254 nm (UV-2102 PC, Shanghai, China). All the processes were carried out for three times [19].

3. Results and Discussion

3.1 Synthesis of P(OVNG-*co*-NVCL)

In this study, galactose-functionalized thermoresponsive double hydrophilic statistical copolymers were prepared by combining enzymatic synthesis with free radical polymerization. N-vinyl caprolactam (NVCL) and galactose were chosen as

the thermoresponsive moiety and bioactive component respectively.

The galactose-functionalized copolymers were prepared by AIBN initiated radical copolymerization of 6-O-vinyl-nonanedioyl-D-galactose (OVNG) with NVCL and fully characterized by ^{1}H NMR and GPC. ^{1}H NMR data (Fig. 1) of the copolymers revealed the absence of vinyl groups and the existence of NVCL and galactose groups. From the ^{1}H NMR spectra, the molar ratio of OVNG to NVCL monomers in the copolymers could be approximately calculated. A series of copolymers with different molecular weights were obtained by varying the OVNG/NVCL feed molar ratios (Table 2).

Characterization data for P(OVNG-*co*-NVCL) are as follows: 5.20-4.30 (1H, br. S, H-6; d, 5H of D-galactose; 1H, -CHCH$_2$-), 4.04-2.80 (3H of D-galactose), 2.48-2.00 (2H, m, H-5; 4H, 2-CH$_2$-), 1.90-1.12 (8H, overlap, H-2, H-3, H-4, H-7; 4H, 2-CH$_2$-). IR (ATR): ν (cm^{-1}): 1721 (O-C=O), 1607 (N-C=O), 3380(-OH).

The chemical composition of the P(OVNG-*co*-NVCL) samples were calculated from the ratio of the peak integrals of the protons of H_{OVNG} (δ 2.48-2.00) with protons of H_{NVCL} (δ 1.90-1.12). It was determined that the OVNG contents (w/w) were 52.38% (OVNG: NVCL=1:1, mol/mol), 36.36% (OVNG: NVCL=1:4, mol/mol), 28.31% (OVNG: NVCL=1:6, mol/mol), and 22.34% (OVNG: NVCL=1:8, mol/mol)

3.2 Lower critical solution temperature (LCST) measurements

To confirm the LCST behavior of P(OVNG-*co*-NVCL) the temperature dependence of the solution transmittance was monitored by UV-visible spectrophotometry (Fig. 2B). It was found that the LCST values of P(OVNG-*co*-NVCL) mol/mol) were 30.4,

32.7, 40.8, and 47.8 ^{o}C respectively when the OVNG content is increased from 22.3%, 28.3%, to 36.3% and 52.3%. The LCST shifts to a higher temperature with the ratio of OVNG due to the increasing hydrophilicity of the glycopolymer [20-21]. The LCST values of P(OVNG-*co*-NVCL) are close to the body temperature, which broadens its use [22].

3.3 Lectin-binding assay

As it was mentioned above, the glycopolymers are able to recognize specific proteins, because glycopolymers with pedant sugar moieties exhibit an enormous advantage compared to single sugar units as the former are capable of multivalent binding to lectins (carbohydrate-binding proteins) in a process known as the "cluster-glycoside effect"[23]. Peanut agglutinin (PNA) can specifically bind galactose residues, so it was used as a model lectin for the preliminary investigations of the biological properties of the galactose-functionalized copolymers [24]. The glycopolymers were incubated with FITC-PNA then dialyzed to remove unbound PNA and analyzed by fluorescence spectroscopy.

Fluorescence methods have been used extensively to study the specific adhesion of lectin with glycopolymers. The lectin-binding activity of P(OVNG-*co*-NVCL) were investigated with FITC-PNA, which can efficiently adhere to copolymers bearing a terminal galactose moiety by carbohydrate-protein affinity. Fluorescence microscopy images of the thermoresponsive glycopolymers are shown in Fig. 3.

Bright green fluorescence attributed to FITC was detected from all types of glycopolymers treated with FITC-PNA, clearly indicating that FITC-PNA binds to the

glycopolymers with galactose branched chain. Different fluorescence images were observed with P(OVNG-*co*-NVCL), with those having a longer length of galactose branch being easily identified and can label the target lectin by means of the clustering effect of carbohydrates and fluorescence from FITC. Fluorescence glycopolymer spots can be observed obviously for P(OVNG-*co*-NVCL), which indicates that P(OVNG-*co*-NVCL) show good lectin-binding activity.

However, the results from the fluorescence of the clusters varied significantly depending on the concentration of the galactose residues. The quantity of clustering for P(OVNG-*co*-NVCL) increases as the OVNG contents decrease from 52.3% to 22.3%. Less OVNG content may affect the binding behavior and lead to considerable clustering. With the decrease in galactose monomer content, other recognition sites of lectin could still identify other glycopolymer molecules. Certainly, more OVNG could increase the density of the fluorescence. (Fig. 3b and Fig. 3c).

3.4 Cytotoxicity assays

MTT cell viability assays were utilized to evaluate the cytocompatibility of the synthesized thermoglycopolymers. The viability of Hela cells seeded onto the tissue culture plates (TCPs) after 1 day of culture in the presence of various formulations of P(OVNG-*co*-NVCL) are shown in Fig. 4A, with the TCPs being used as a control. P(OVNG-*co*-NVCL, 1:4) showed approximately similar cell viability to P(OVNG-*co*-NVCL, 1:6). Cell viability varies from 94% to 90% for P (OVNG-*co*-NVCL, 1:1) and littler higher for P(OVNG-*co*-NVCL, 1:8) from 98% to 92%. This might be ascribed to the structure status in the medium; more NVCL or

galactose could provide an appropriate microenvironment for cell attachment and migration. P(OVNG-*co*-NVCL) is non-toxic even in the highest concentration of 100 mg/L. The cell viability cultured on the five materials exceeded 75% ($P>0.05$, no significant difference), thus all five glycopolymers have relatively good cytocompatibility, which is essential for their biomedical applications.

P(OVNG-*co*-NVCL, 1:4) has a better biological recognition ability compared to other glycopolymers and the LCST value of the polymer is also similar to body temperature. So this polymer was selected for further investigation using different concentrations in a second MTT assay and the data in Fig 4B shows that P(OVNG-*co*-NVCL, 1:4) has low cytotoxity.

3.5 Morphologies of nanofiber mats

Thermoresponsive glycopolymers have been reported to be promising drug delivery vehicle because of their good biocompatibility, non-toxicity and temperature controlled release of drugs [25]. According to the work discussed above, P(OVNG-*co*-NVCL, 1:4) showed a LCST value (40.7 ^{o}C) close to the temperature of the human , a better lectin-binding ability and lower cytotoxicity and consequently the P(OVNG-*co*-NVCL, 1:4) was chosen for sustained drug release studies. The electrospun P(OVNG-*co*-NVCL) and FA/P(OVNG-*co*-NVCL) nanofibers were fabricated and characterized by SEM. The uniform fibrous structures of P (OVNG-*co*-NVCL) material chosen for optimization studies were dependent on various parameters including applied high voltage, electrospinning distance and

solution concentration [26].

Fig. 5A shows SEM micrographs of the nanofiber mats formed using P(OVNG-*co*-NVCL). In the nine pictures the P(OVNG-*co*-NVCL) nanofibers displayed a smooth and flat morphology and relatively uniform diameter distribution. Fig. 5B shows the average diameter distribution values of the nanofibers based on a selection of electron micrographs of each material (100 fibers). The morphologies of the nanofibers of FA/P(OVNG-*co*-NVCL) are different from P(OVNG-*co*-NVCL) (Fig. 5A) since more particles exist in the FA-loaded nanofibers as the FA content is increased from 5% to 20%, compared with 0%. [27-28].

3.6 Thermogravimetric analysis of glycopolymers

The thermal stability of the FA loaded glycopolymers was assessed by thermogravimetry. The analyses were carried out at temperatures ranging between 0 and 900 ^{o}C. Fig. 6B presents the TG diagrams of the FA, P(OVNG-*co*-NVCL) and P(OVNG-*co*-NVCL)/FA. The degradation of the P(OVNG-*co*-NVCL)/FA occurs following four inflexions of the TG curves.

3.7 In vitro drug release

In order to investigate in vitro drug release, ferulic acid (4-hydroxy-3-methoxy cinnamic acid, FA), a natural antioxidant with potential health benefits against cardiovascular problems, inflammatory diseases and certain cancers) was selected and loaded onto the nanofibers as drug substrate. Figure 6C shows FA release profiles from electrospun P(OVNG-*co*-NVCL) nanofibers with different FA proportions at

different temperatures of 20 ^{o}C and 40 ^{o}C. Experiments were performed in triplicate and error bars indicate the standard deviation. The release kinetics from the sample shows two stages: an initial fast release before the inflections (stage I) followed by a slow and constant release (stage II) [29]. In stage I, there were initial rapid release from the electrospun mats, then the release ceased and the remainder of the drug was released in stage II. Xu et al. [30] had found that the drug release behavior was related to the distribution of drug in the fiber mats. In the process of electrospinning, FA molecules exist both at the outer and inner surface of the nanofiber mats [31].

During the release processes, FA present on the surface dissolved in PBS solution. Thereafter, the FA present within the mat diffused into PBS along with the dissolution of P(OVNG-*co*-NVCL), but the quantity was very small and the process was very slow. The encapsulation efficiencies of FA in P(OVNG-*co*-NVCL) nanofibers electrospun from blend solution of P(OVNG-*co*-NVCL) were found to be 75.4 ± 3.5% for 5% FA loaded; 82.3 ± 3.6% for 10% FA loaded; and 85.9 ± 3.4% for 20% FA loaded.

For P(OVNG-*co*-NVCL) with 10% FA at 20 ^{o}C, there was an initial burst release 96.8% within 8 h (Fig.9). In the following 18.5 h to 72 h, the amount of drug released reached 97.7%. In sharp contrast, the drug loaded P(OVNG-*co*-NVCL) composite nanofibers showed a relatively sustained FA release from P(OVNG-*co*-NVCL) /FA. Around 15.1%, 18.3% and 15.9% of FA were released from 5 wt%, 10 wt%, 20 wt% P(OVNG-*co*-NVCL) /FA nanofibers at 40 ^{o}C, respectively within the first 8 h. And then a plateau was reached after 28 h with a release percentage of > 50% for these

three mix electrospun P(OVNG-*co*-NVCL) /FA nanofibers with different FA proportions. The release percentages of P(OVNG-*co*-NVCL) /FA (10 wt %) nanofibrous mats at 40 ^{o}C at 72 h was much lower than that of the P(OVNG-*co*-NVCL) /FA (10 wt %) nanofibers within the 8 h at 20 ^{o}C. The sustained release profile of FA from P(OVNG-*co*-NVCL)/FA nanofibers is due to the fact that the soluble structure affect the kinetics of drug release. [32].

4. Conclusion

In summary, thermoresponsive double-hydrophilic glycopolymer nanofibers have been fabricated. It was found that the LCST values of P(OVNG-*co*-NVCL), close to human body temperature, may be made simply by adjusting the proportion of OVNG and NVCL in the polymerization process. P(OVNG-*co*-NVCL) showed low cytotoxity in MTT cell viability assays. Moreover，FA-loaded DHG nanofibers were successfully prepared using an electrospinning process. In vitro studies showed that drug release was highly dependent upon the temperature, crucially, upon the polymer forming filament. Therefore, P(OVNG-*co*-NVCL) nanofibers may have a potential application in the design of temperature controlled drug release formulations.

Acknowledgments.

This investigation was supported by the National Natural Science Foundation of China (No.21303014), the State Key Laboratory for the Modification of Chemical

Fibers and Polymer Materials, Key Laboratory of Science & Technology of Eco-Textile，Donghua University.

References

[1] von der Ehe, C., Czaplewska, J. A., Gottschaldt, M., Schubert. Synthesis of thermoresponsive glycopolymers via ATRP of N-isopropylacrylamide and N-allylacrylamide and subsequent thiol–ene reaction, European Polymer Journal 49 (2013) 2660-2669.

[2] Canbolat M. F., Celebioglu A., Uyar T. Drug delivery system based on cyclodextrin-naproxen inclusion complex incorporated in electrospun polycaprolactone nanofibers. Colloids and Surfaces B Biointerfaces, 115 (2014) 15-21.

[3] Wei, H., Zhang, X. Z., Cheng, H., Chen, W. Q., Cheng, S. X., Zhuo, R. X. Self-assembled thermo-and pH responsive micelles of poly (10-undecenoic acid-b-N-isopropylacrylamide) for drug delivery. Journal of controlled release 116 (2006) 266-274.

[4] Graillot A., Bouyer D., Monge S., Robin, J. J., Faur C. Removal of nickel ions from aqueous solution by low energy-consuming sorption process involving thermosensitive copolymers with phosphonic acid groups. Journal of Hazardous Materials, 15 (2013) 507–515.

[5] S. G. Kumbar, R. James, S. P. Nukavarapu, C. T. Laurencin, Electrospun nanofiber scaffolds: engineering soft tissues, Biomedical Materials 3 (2008) 034002.

[6] K. Madhusudana Rao, B. Mallikarjuna, K.S.V. Krishna Rao, S. Siraj, K. Chowdoji

Rao, M.C.S. Subha. Novel thermo/pH sensitive nanogels composed from poly(N-vinylcaprolactam) for controlled release of an anticancer drug. Colloids and Surfaces B: Biointerfaces 102 (2013) 891– 897.

[7] Sabrina Belbekhouche, Virginie Dulong, Luc Picton, Didier Le Cerf. Saccharide effect on the LCST property of a polyether: Influence of structure and length. Colloids and Surfaces A: Physicochemical and Engineering Aspects 428 (2013) 25– 31.

[8] Henna Vihola, Antti Laukkanen, Jouni Hirvonen, Heikki Tenhu. Binding and release of drugs into and from thermosensitive poly(N-vinylcaprolactam) nanoparticles. European Journal of Pharmaceutical Sciences 16 (2002) 69–74.

[9] Nagihan Okutan, Pınar Terzi, Filiz Altay. Affecting parameters on electrospinning process and characterization of electrospun gelatin nanofibers. Food Hydrocolloids 39 (2014) 19-26.

[10] Ting, S. S., Min, E. H., Escalé, P., Save, M., Billon, L., Stenzel, M. H. Lectin recognizable biomaterials synthesized via nitroxide-mediated polymerization of a methacryloyl galactose monomer. Macromolecules, 42 (2009) 9422-9434.

[11] Sun K, Bligh S W A, Nie H, et al. Lectin recognizing thermoresponsive double hydrophilic glycopolymer micelles by RAFT polymerization. RSC Advances, 66 (2014) 34912-34921.

[12] Hassani L N, Hendra F, Bouchemal K. Auto-associative amphiphilic polysaccharides as drug delivery systems. Drug discovery today 11 (2012) 608-614.

[13] Qi, R., Guo, R., Zheng, F., Liu, H., Yu, J., Shi, X. Controlled release and antibacterial activity of antibiotic-loaded electrospun halloysite/poly (lactic-co-glycolic acid) composite nanofibers[J]. Colloids and Surfaces B: Biointerfaces, 110 (2013) 148-155.

[14] L. Y. Huang, Branford-White C, X. X. Shen, D. G. Yu, L. M. Zhu Time-engineeringed biphasic drug release by electrospun nanofiber meshes. International journal of pharmaceutics, 1 (2012) 88-96.

[15] W. S. Yu, Q. L. Ma, X. L. Li, X. T. Dong, J. X. Wang, G. X. Liu. One-pot coaxial electrospinning fabrication and properties of magnetic-luminescent bifunctional flexible hollow nanofibers. Materials Letters, 120 (2014) 126–129.

[16] C. Y. Chen, T. H. Kim, W. C. Wu, C. M. Huang, H. Wei, Christopher W. Mount, Y. Q. Tian, S. H. Jang, Suzie H. Pun, Alex K.-Y. Jen. pH-dependent, thermosensitive polymeric nanocarriers for drug delivery to solid tumors. Biomaterials 34 (2013) 4501-4509.

[17] L. Wang, Williams, G. R., H. L Nie, J. Quan, L. M. Zhu. Electrospun glycopolymer fibers for lectin recognition. Polym Chem, 8 (2014) 3009-3017.

[18] Ana-Maria Pan, Vasile Gherman, Paula Sfîrloag, Geza Bandur, Liliana-Marinela Stefan, Marcel Popa, Lucian-Mircea Rusnac. Thermal stability and biodegradation of novel D-mannose based glycopolymers. Polymer Testing 31 (2012) 384–392.

[19] L. Q. Chen, L. M. Zhang, J. J. Chen, J. Yang, R. Li. Self-assembly and drug delivery behaviors of a novel thermo-sensitive block glycopolymer. Chinese Science Bulletin, 36 (2010) 4187-4196.

[20] Eissa A. M., Khosravi E. Synthesis of a new smart temperature responsive glycopolymer via click-polymerisation. European Polymer Journal, 47 (2011) 61-69.

[21] Marya Ahmed, Ravin Narain. The effect of molecular weight, compositions and lectin type on the properties of hyperbranched glycopolymers as non-viral gene delivery systems. Biomaterials 33 (2012) 3990-4001.

[22] Garnier, S., Laschewsky, A. Synthesis of new amphiphilic diblock copolymers and their self-assembly in aqueous solution. Macromolecules, 38 (2005) 7580-7592.

[23] Noble G T, Flitsch S L, Liem K P, et al. Assessing the cluster glycoside effect during the binding of concanavalin A to mannosylated artificial lipid rafts. Organic & biomolecular chemistry, 24 (2009) 5245-5254.

[24] Y. Li, J. Quan, Christopher Branford-White, Gareth R. Williams, J. X. Wu, L. M. Zhu. Electrospun polyacrylonitrile-glycopolymer nanofibrous membranes for enzyme immobilization. Journal of Molecular Catalysis B: Enzymatic 76 (2012) 15-22.

[25] Kenawy E R, Abdel-Hay F I, El-Newehy M H, et al. Controlled release of ketoprofen from electrospun poly (vinyl alcohol) nanofibers. Materials Science and Engineering: A 1 (2007) 390-396.

[26] Che A. F., Huang X J, Xu Z K. Polyacrylonitrile-based nanofibrous membrane with glycosylated surface for lectin affinity adsorption. Journal of Membrane Science,

1 (2011) 272-277.

[27] Y. Su, Q. Q. Su, W. Liu, Marcus Lim, Jayarama Reddy Venugopal, Xiumei Mo, Seeram Ramakrishna, Salem S. Al-Deyabe, Mohamed El-Newehy. Controlled release of bone morphogenetic protein 2 and dexamethasone loaded in core–shell PLLACL–collagen fibers for use in bone tissue engineering. Acta Biomaterialia 8 (2012) 763-771.

[28] Q. Y. Meng, Amranul Haque, Bayar Hexig, Toshihiro Akaike. The differentiation and isolation of mouse embryonic stem cells toward hepatocytes using galactose-carrying substrata. Biomaterials 33 (2012) 1414-1427.

[29] L. Y. Huang, D. G. Yu, Branford-White C, L. M. Zhu. Sustained release of ethyl cellulose micro-particulate drug delivery systems prepared using electrospraying. Journal of Materials Science 3 47(2012): 1372-1377.

[30] T. Xu, S. H. Wang, Z. Z. Shao. O-methyl-free N, N, N-trimethyl chitosans with various molecular weights as gene carriers. Journal of Controlled Release 172 (2013) 98-124.

[31] X. Wang, X. Geng, L. Ye, A. Y. Zhang, Z. G. Feng. Synthesis and characterization of novel glucose- and lactose-containing methacrylate-based radiopaque glycopolymers. Reactive & Functional Polymers 69 (2009) 857-863.

[32] H. Zhang, S. F. Lou, Williams G. R., Branford-White C., H. L. Nie, J. Quan, Zhu L. M. A systematic study of captopril-loaded polyester fiber mats prepared by electrospinning. International journal of pharmaceutics, 1 (2012) 100-108.

Table 1. The specific situation of L9 (3) ^{4} orthogonal of electrospinning

Sample ID	Voltage (kV)	Collection Distance (cm)	Feed rates (mL/h)	Solution concentration (wt %)
1	12	12	0.3	35
2	12	15	0.7	37
3	12	18	0.5	39
4	13.5	15	0.5	35
5	13.5	18	0.3	37
6	13.5	12	0.7	39
7	15	18	0.7	35
8	15	12	0.5	37
9	15	15	0.3	39

Table 2. Characterization data for the polymers (SD, n=3)

Sample ID	OVNG/NVCL (mol/mol)	M_n [a] $\times 10^{-4}$ (D_a)	M_w/M_n [a]	OVNG content [b] (w/w %)
a	1/1	4.189	1.092	52.38
b	1/4	3.864	1.537	36.36
c	1/6	3.767	1.062	28.31
d	1/8	1.867	1.209	22.34

[a] Determined by GPC

[b] Determined by ^{1}H NMR measurements in D_2O

Fig. 1(A) The synthesis of P(OVNG-*co*-NVCL) by controllable regioselective enzymatic transesterification and free radical polymerization; (B)^{1}H NMR spectra of (a) P(OVNG-*co*-NVCL) and (b) monomer OVNG

Fig. 2 (A) Infrared spectra of P(OVNG-*co*-NVCL) at various ratios [a. P(OVNG-*co*-NVCL, 1:8), b. P(OVNG-*co*-NVCL, 1:6), c P(OVNG-*co*-NVCL, 1:4), d. P(OVNG-*co*-NVCL, 1:1) and e. OVNG] (B) Temperature dependence of the transmittance of aqueous solutions of P(OVNG-*co*-NVCL) products

Fig. 3 Images of PNA-FITC binding with thermoresponsive P(OVNG-*co*-NVCL). Molar input ratios of OVNG to NVCL: (a) 1: 1; (b) 1: 4; (c) 1: 6; (d) 1: 8

Fig. 4 (A) Proliferation of Hela cells seeded onto tissue culture plates (TCP) in the presence of P(OVNG-*co*-NVCL); (B) on P(OVNG-*co*-NVCL, 1:4) after 1 day's culture label the figure with A and B (SD, n=3)

Fig. 5 (A) SEM images of the fiber mats containing various amounts of FA. The concentration of P(OVNG-*co*-NVCL) was fixed at 35wt% (1-3), 37wt% (4-6), 39wt% (7-9), all scale labels are 30 μm. (B) The average diameter distribution values of nanofibers

Fig. 6 (A) Representative morphologies of different loaded FA/P(OVNG-*co*-NVCL) nanofibers. (FA content increased from 5% to 20%, compared with 0%); (B) TG diagram of the FA, P(OVNG-*co*-NVCL) and P(OVNG-*co*-NVCL)/FA; (C) Sustained release of FA from P(OVNG-*co*-NVCL)/FA nanofibers at 20 ^{o}C and 40 ^{o}C (SD, n=3)

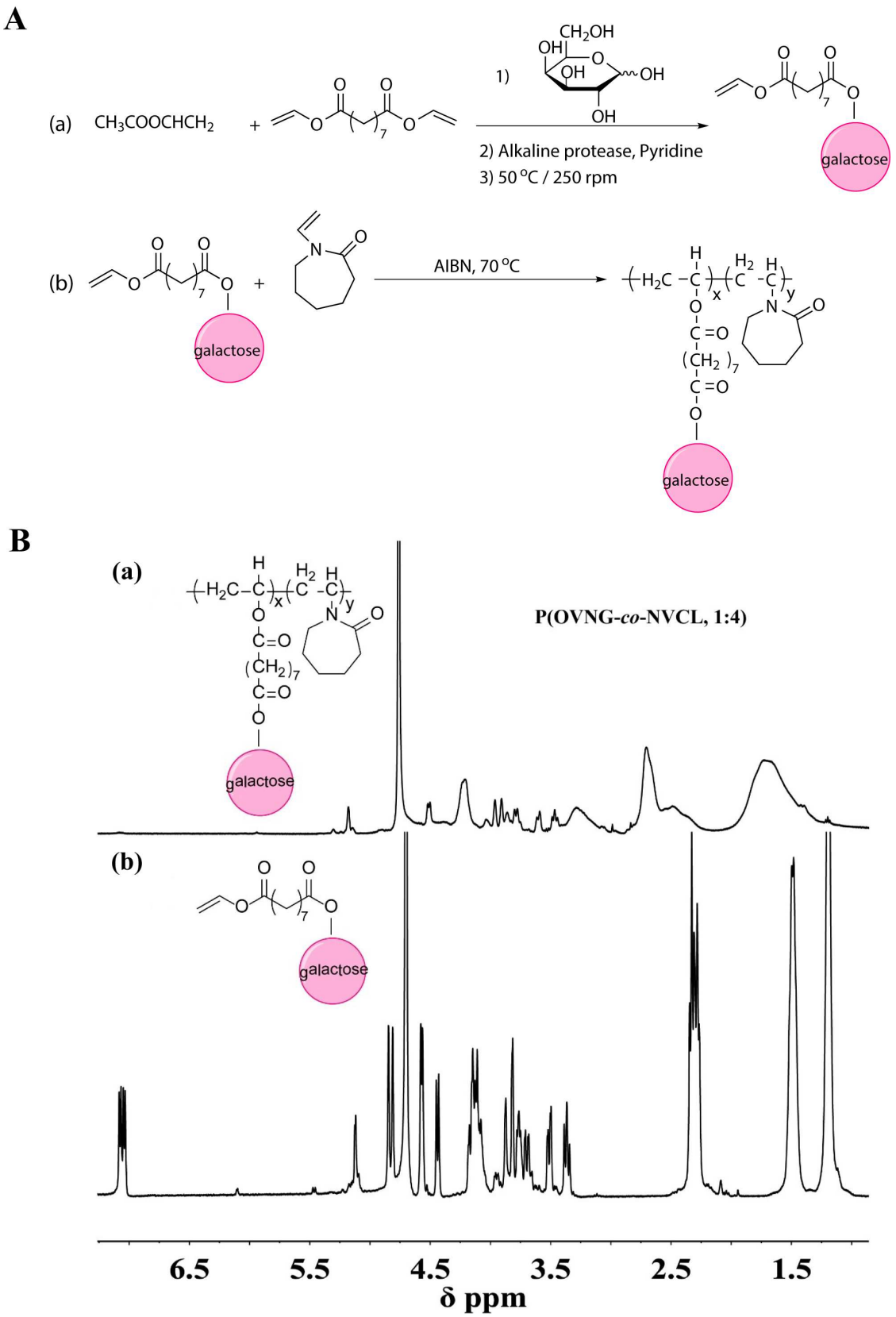

Fig. 1(A) The synthesis of P(OVNG-*co*-NVCL) by controllable regioselective enzymatic transesterification and free radical polymerization; (B)1H NMR spectra of (a) P(OVNG-co-NVCL) and (b) monomer OVNG

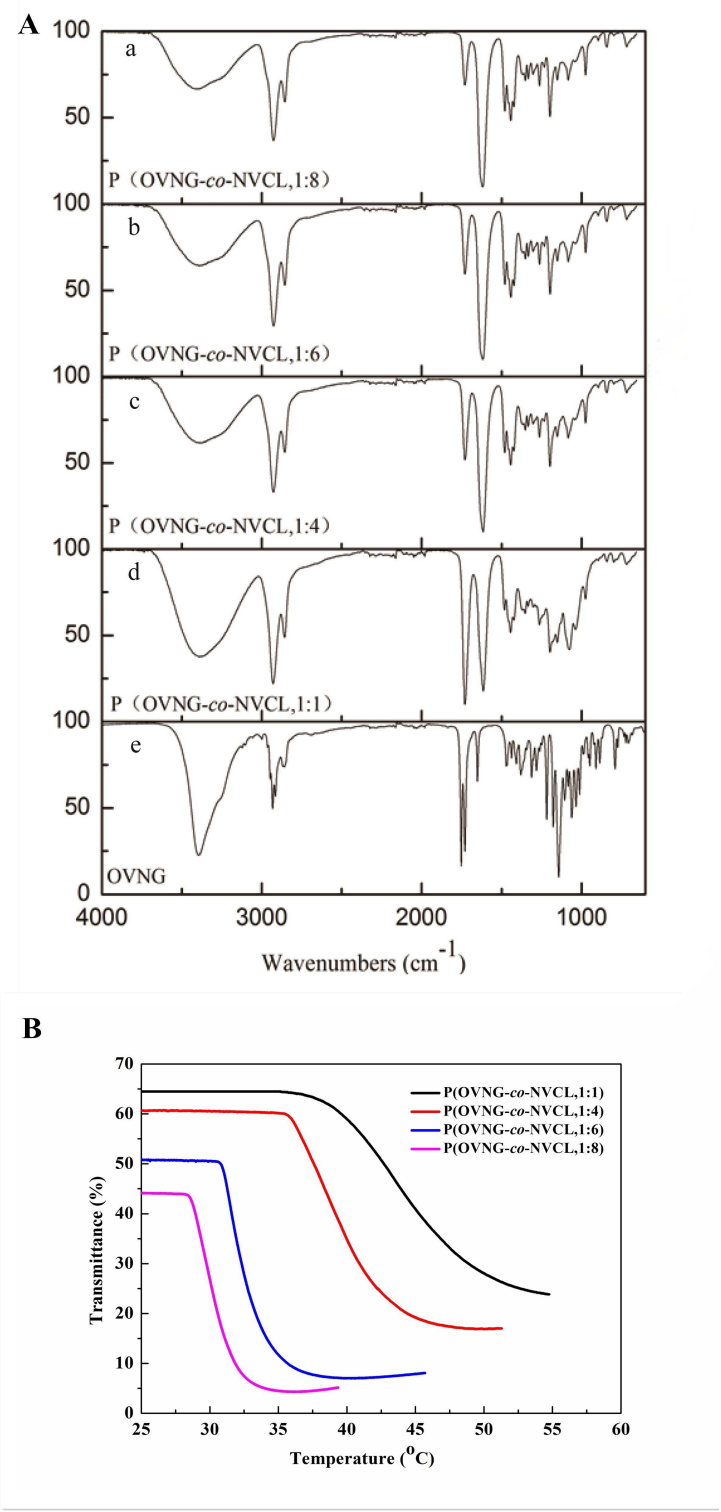

Fig. 2 (A) Infrared spectra of P(OVNG-*co*-NVCL) at various ratios [a. P(OVNG-*co*-NVCL, 1:8), b. P(OVNG-*co*-NVCL, 1:6), c P(OVNG-*co*-NVCL, 1:4), d. P(OVNG-*co*-NVCL, 1:1) and e. OVNG] (B) Temperature dependence of the transmittance of aqueous solutions of P(OVNG-*co*-NVCL) products

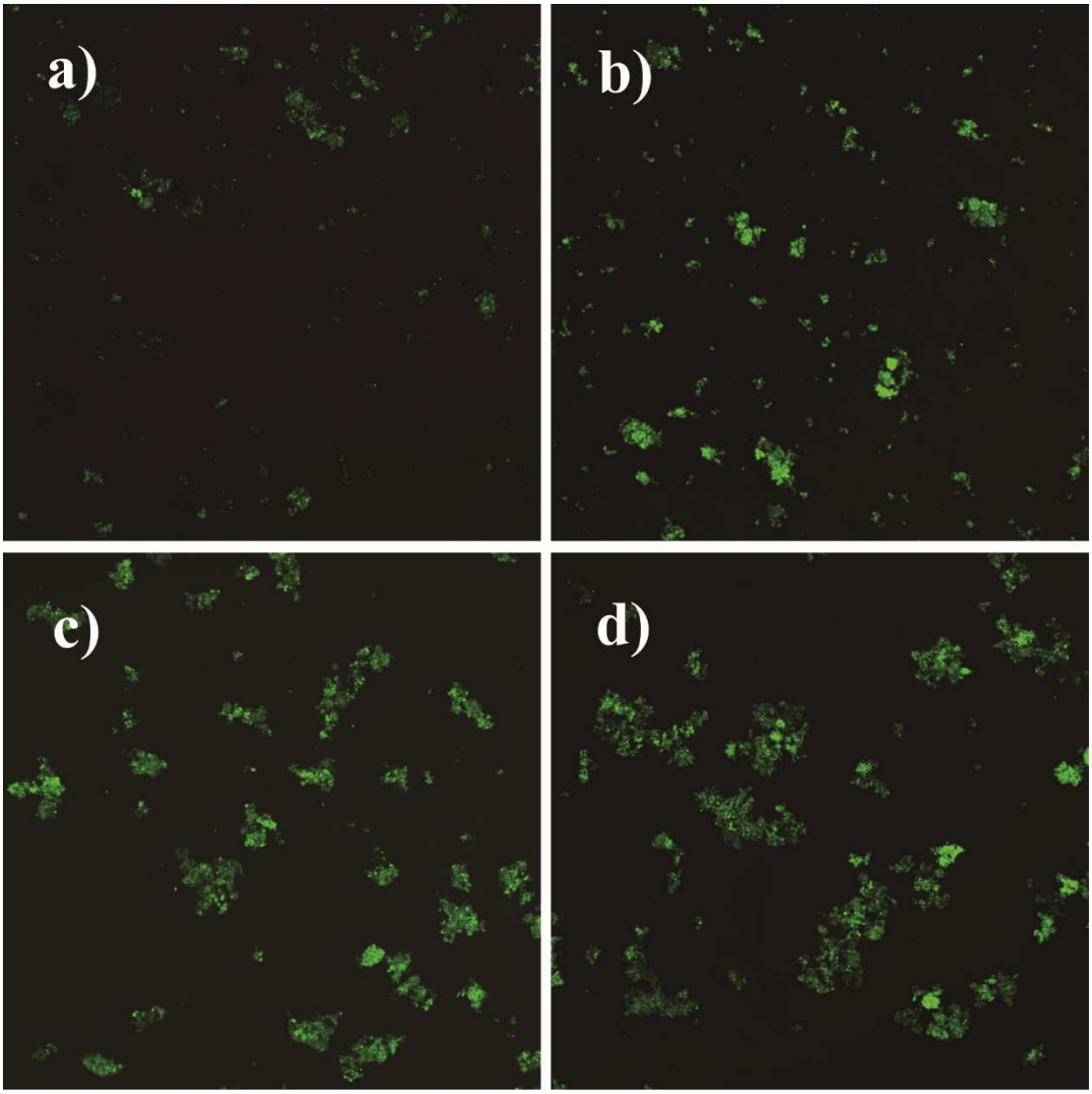

Fig. 3 Images of PNA-FITC binding with thermoresponsive P(OVNG-*co*-NVCL). Molar input ratios of OVNG to NVCL: (a) 1: 1; (b) 1: 4; (c) 1: 6; (d) 1: 8

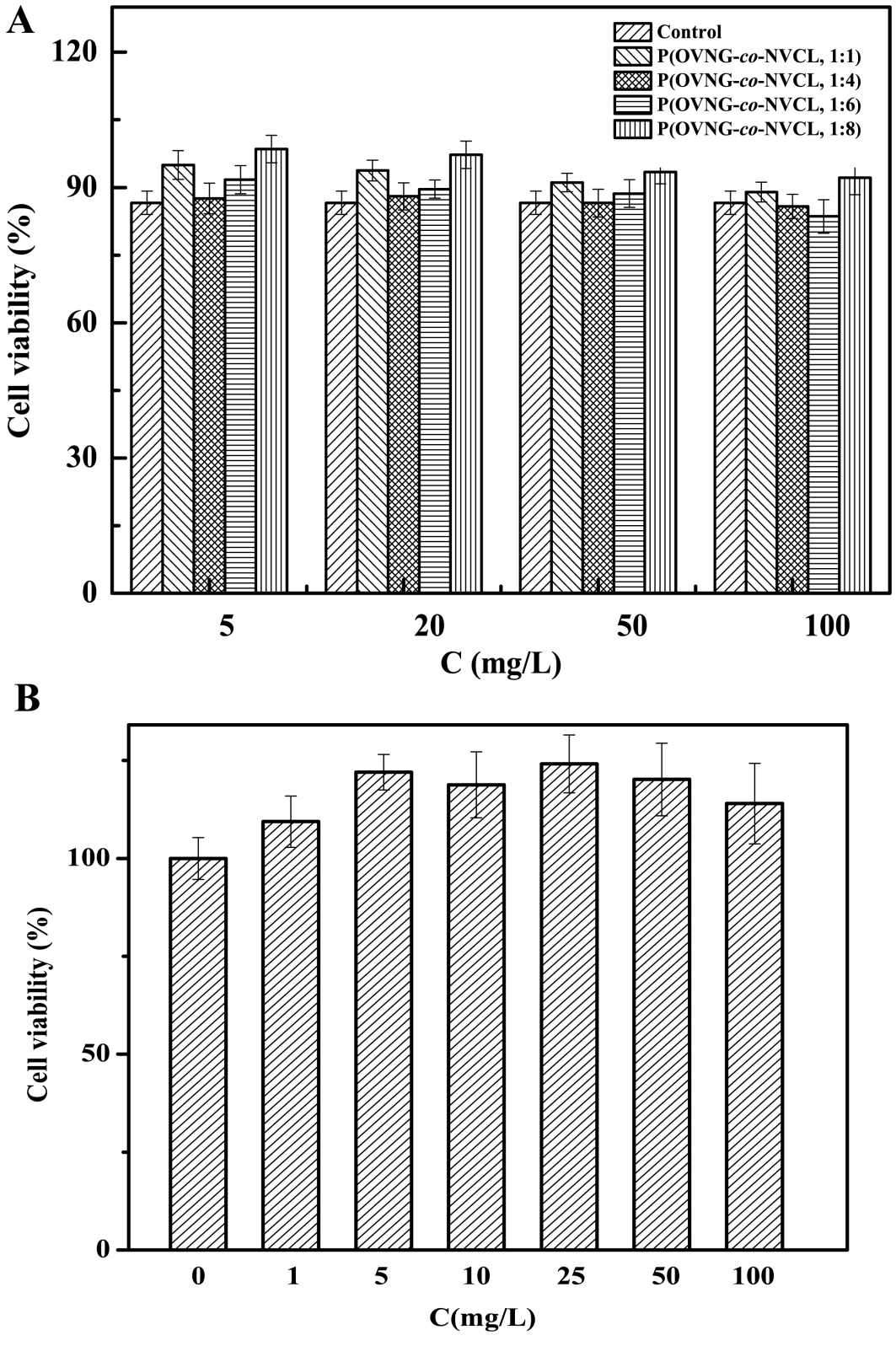

Fig. 4 (A) Proliferation of Hela cells seeded onto tissue culture plates (TCP) in the presence of P(OVNG-*co*-NVCL); (B) on P(OVNG-*co*-NVCL, 1:4) after 1 day's culture label the figure with A and B (SD, n=3)

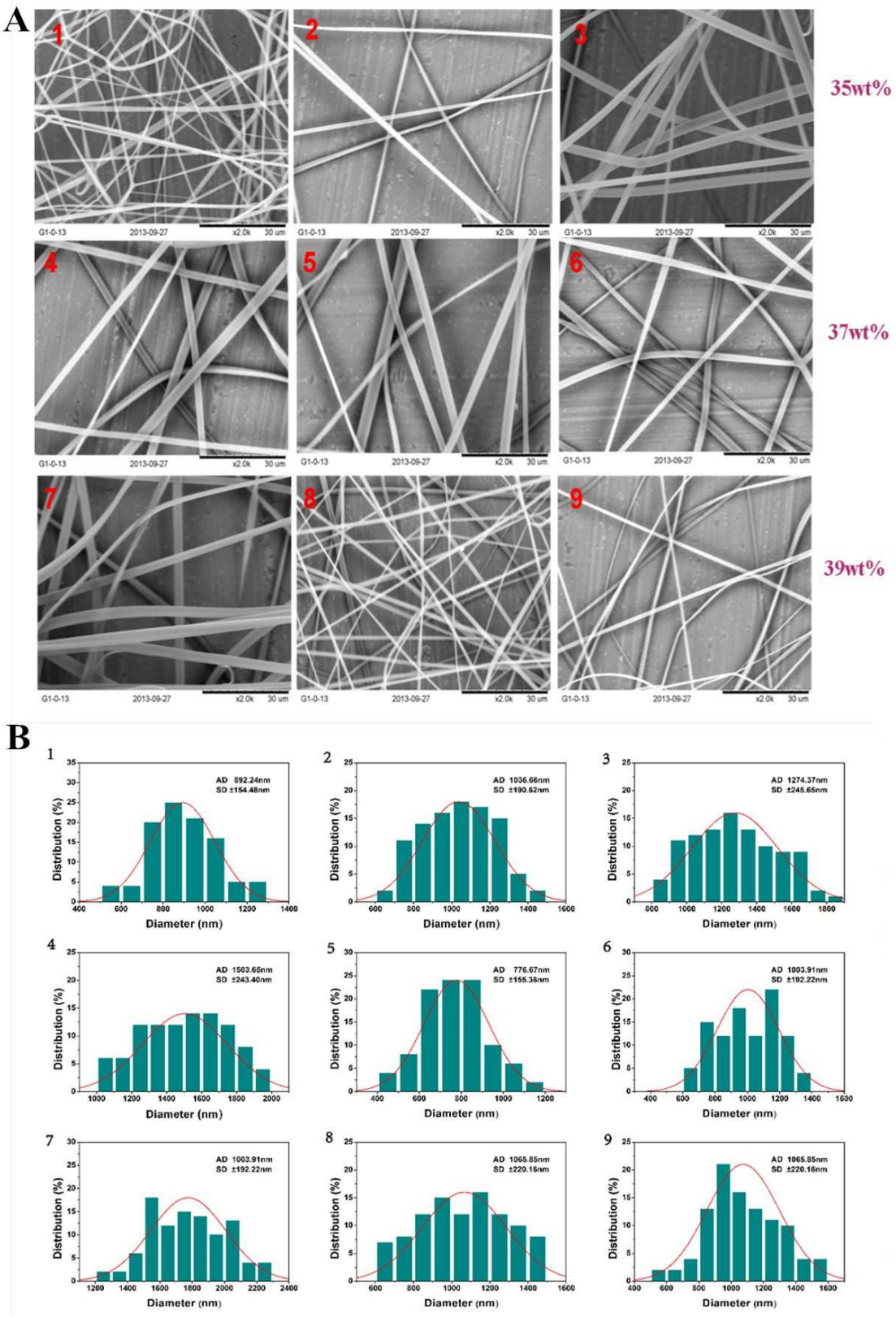

Fig. 5 (A) SEM images of the fiber mats containing various amounts of FA. The concentration of P(OVNG-*co*-NVCL) was fixed at 35wt% (1-3), 37wt% (4-6), 39wt% (7-9), all scale labels are 30 μm. (B) The average diameter distribution values of nanofibers

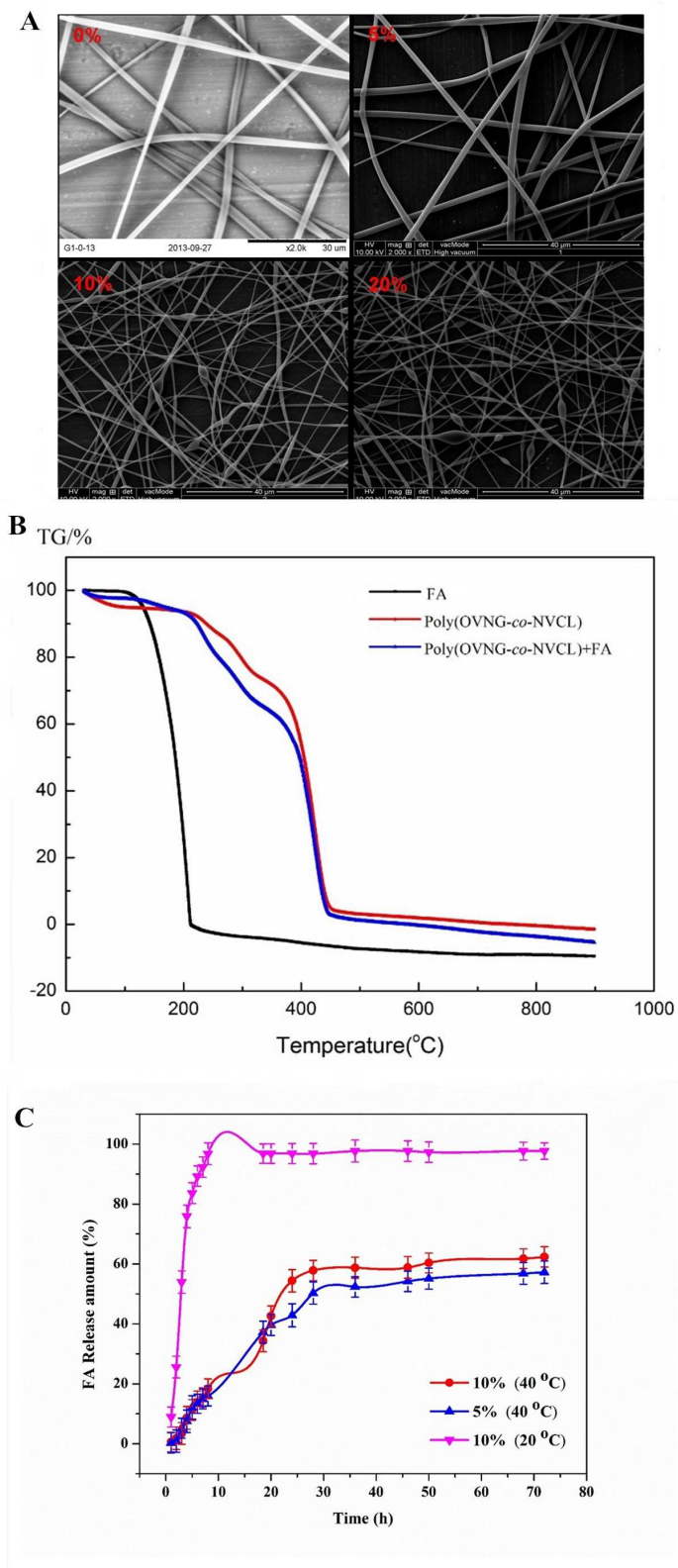

Fig. 6 (A) Representative morphologies of different loaded FA/P(OVNG-co-NVCL) nanofibers. (FA content increased from 5% to 20%, compared with 0%); (B) TG diagram of the FA, P(OVNG-co-NVCL) and P(OVNG-co-NVCL)/FA; (C) Sustained release of FA from P(OVNG-co-NVCL)/FA nanofibers at 20 oC and 40 oC (SD, n=3)